

# Using vibration patterns to provide impact position information in haptic manipulation of virtual objects

Jean Sreng<sup>1</sup>, Anatole Lécuyer<sup>2</sup>, and Claude Andriot<sup>3</sup>

<sup>1</sup> CEA / INRIA,  
IRISA, Campus de Beaulieu, 35042 Rennes, France

[jean.sreng@inria.fr](mailto:jean.sreng@inria.fr)

<sup>2</sup> INRIA / IRISA,  
Campus de Beaulieu, 35042 Rennes, France

[anatole.lecuyer@irisa.fr](mailto:anatole.lecuyer@irisa.fr)

<sup>3</sup> CEA,  
18 Route du Panorama, BP6, 92265 Fontenay-aux-Roses  
[claude.andriot@cea.fr](mailto:claude.andriot@cea.fr)

**Abstract.** While standard closed haptic control loop used in haptic simulation of rigid bodies are bounded to low frequency force restitution, event-based or open-loop haptic, by superimposing a high-frequency transient force pattern, can provide a realistic feeling of the impact. This high-frequency transient can provide the user with rich information about the contact such as the material properties of the object. Similarly, an impact on different locations of an object produces different vibration patterns that can be used to determine the impact location.

This paper investigates the use of such high-frequency vibration patterns to provide impact position information on a simulated long rod held by the edge. We propose in this paper different vibration pattern models to convey the position information: a realistic model based on a numerical simulation of a beam and three empirical simplified models based on exponentially decaying sinusoids. A preliminary evaluation has been conducted with 15 participants. Taken together, our results showed that the users are able to associate vibration information with impact position efficiently.

**Key words:** open-loop haptic, impact, vibration patterns, contact position

## 1 Introduction

Haptic simulation of virtual rigid bodies is increasingly used in various areas of virtual reality such as virtual prototyping, assembly/maintenance simulations, games, etc. In such simulations, impact information is an important feature as it warns the user about a new contact on the manipulated object. However, due to limited computational resources, sensor resolution and stability issues, the

standard haptic closed control loop, bounded to low frequency force restitution, cannot render stable realistic impacts.

While manipulating an object in a real environment, the human hand is able to feel high-frequency responses, up to several hundred Hertz, through different corpuscles located in the skin [2] together with low-frequency forces perceived in the muscles and tendons of the arm. These high-frequency responses resulting of the physical interaction between the manipulated object and the environment can provide the person manipulating with information about the material properties or the surface texture of the objects for instance.

The event-based haptic or open-loop approach has been proposed to augment the standard haptic feedback with high-frequency impact transients. This rendering technique, stimulating the high-frequency receptors in the hand provides a more realistic feeling of the impact and can convey material properties information.

In this paper, we investigate how this high-frequency force transient can be used to convey position information. An impact on a manipulated object creates high-frequency propagating vibrations that produce different transient patterns in the hand depending on the impact location on the object. These high-frequency patterns are expected to help the user in determining the impact location. We propose to test this hypothesis on a simple long rod held by one edge as described in Section 3. We propose different vibration pattern models to provide the impact location: a realistic pattern based on the numerical simulation of a beam and several empirical simplified patterns based on exponentially decaying sinusoids.

A preliminary experiment described in Section 4 has been conducted to test the ability of users to discriminate different contact locations using these different vibration patterns. The results of this study are presented and discussed in Sections 5 and 6, followed by concluding remarks in Section 7.

## 2 Related work

Among the different sensory inputs used during human manipulation, we can differentiate the proprioceptive perception and the tactile perception. Proprioception is essential during the manipulation through the forces and positions perceived in the muscles and tendons. These sensory inputs, strongly correlated with the human motion are restricted to a low-frequency resolution. In contrast the tactile perception, through the different corpuscles found in the skin [2] can detect signals up to 1kHz with the highest sensitivity around 250Hz. These mechanoreceptors are also able to differentiate some complex signals [1].

Such high-frequency vibrations occur when tapping stiff materials like steel or glass [7] up to several kHz. It has been shown in telemanipulation tasks that feeding back to the operator such high-frequency signals improves the performance [4].

These high-frequency patterns have also been used in the event-based haptic approach to improve the haptic simulation of impact. This approach has

been proposed to augment the standard haptic feedback with high-frequency impact transient. This impact transient can be approximated as an exponentially decaying sinusoid which frequency depends on the material [9]. This kind of transient has been found to improve the realism of the impact and allow the user to differentiate between several materials like wood, rubber or steel [8]. More complex transients, measured on real materials have also been proposed [6]. These complex transients achieve a higher realism than the exponentially decaying sinusoids.

Vibrations patterns have also been proposed for the simulation of a rolling object inside a hand-held tube [10]. This vibration pattern together with motor control and audio output allows the user to discriminate between the lengths of different virtual tubes. The blind haptic perception of a rod length has also been studied [3]. In these experiments, the subject moved the rod and used proprioceptive cues such as torques and inertia to determine the length.

### 3 Vibration patterns to determine the impact position

High-frequency transient, used to improve the realism of a simulated impact, can allow the user to determine the manipulated material. However, little is known about the user's ability to perceive the impact location through the different vibration patterns that are generated by different impact locations. In this paper, we propose to test several vibration pattern models to convey the impact position information on a very simple manipulation task.

The manipulation task we chose consists in a long virtual rod held by the hand at one edge that can be only moved along the vertical axis. While moving down, the rod can impact a virtual obstacle that can be placed at different locations along the length of the rod. At the moment of the impact, the user perceives the proprioceptive cue of contact (the rod cannot move down any further) and the tactile cue of the vibrations generated by the impact and propagating along the rod.

In the following section we will detail the physical model we chose to determine the vibrations generated by an impact on the rod.

#### 3.1 The Euler-Bernoulli beam

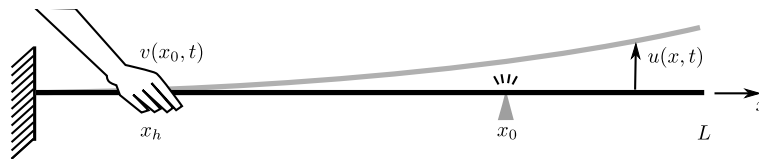


Fig. 1. The Euler-Bernoulli beam

We chose to approximate the rod held by the hand at one edge by a cantilever Euler-Bernoulli beam (thus neglecting the hand impedance). The Euler-Bernoulli beam model is simple and accurate enough if the order of the length to thickness ratio is 20 or more. The following equation describes the beam deflexion  $u$  on the vertical axis at some position  $x$  along the beam and time  $t$  (see Figure 1):

$$EI \frac{\partial^4 u}{\partial x^4} + \lambda \frac{\partial u}{\partial t} + \rho \frac{\partial^2 u}{\partial t^2} = 0 \quad (1)$$

with  $E$  the Young's modulus,  $I$  the second moment of area,  $\lambda$  the viscous resistance and  $\rho$  the linear mass. This equation leads to :

$$\left\{ \begin{array}{l} u(x, t) = \tilde{u}(x) f(t) \\ \frac{d^4 \tilde{u}}{dx^4} - \beta^4 \tilde{u} = 0 \\ \frac{d^2 f}{dt^2} + \frac{\lambda}{\rho} \frac{df}{dt} + \omega_0^2 f = 0 \end{array} \right. \quad (2)$$

$$\frac{d^4 \tilde{u}}{dx^4} - \beta^4 \tilde{u} = 0 \quad (3)$$

$$\frac{d^2 f}{dt^2} + \frac{\lambda}{\rho} \frac{df}{dt} + \omega_0^2 f = 0 \quad (4)$$

These equations integrate (on the underdamped condition) to :

$$\tilde{u}(x) = A \cos(\beta x) + B \sin(\beta x) + C \cosh(\beta x) + D \sinh(\beta x) \quad (5)$$

$$f(t) = e^{-\frac{\lambda}{2\rho} t} \sin(\omega t + \phi) \quad (6)$$

with :

$$\beta^4 = \frac{\rho}{EI} \omega_0^2 \quad (7)$$

$$\omega^2 = \sqrt{\omega_0^2 - \frac{\lambda^2}{4\rho^2}} \quad (8)$$

The different parameters  $A$ ,  $B$ ,  $C$ ,  $D$ ,  $\beta$  are determined with the boundary conditions of a cantilever beam of length  $L$ :

$$\tilde{u}(0) = \frac{d\tilde{u}}{dx}(0) = \frac{d^2\tilde{u}}{dx^2}(L) = \frac{d^3\tilde{u}}{dx^3}(L) = 0 \quad (9)$$

which lead to :

$$A = -C = k \quad (10)$$

$$D = -B = k \frac{\cos(\beta L) + \cosh(\beta L)}{\sin(\beta L) + \sinh(\beta L)} = k\alpha \quad (11)$$

$$0 = \cos(\beta L) \cosh(\beta L) + 1 \quad (12)$$

So the general solution basis is :

$$\tilde{u}_n(x) = \cos(\beta_n x) - \cosh(\beta_n x) + \alpha_n (\sinh(\beta_n x) - \cosh(\beta_n x)) \quad (13)$$

$$f_n(t) = e^{-\frac{\lambda}{2\rho} t} \sin(\omega_n t + \phi_n) \quad (14)$$

with  $\beta_n$  solutions of Equation 12 in increasing order and  $\omega_n$  determined by Equations 7 and 8. So that :

$$u(x, t) = \sum_n A_n \tilde{u}_n(x) f_n(t) \quad (15)$$

$A_n$  and  $\phi_n$  are determined by the initial conditions :

$$\begin{cases} u(x, 0) = 0 \\ \frac{\partial u}{\partial t}(x, 0) = g(x_0, x) = e^{-\left(\frac{x-x_0}{\sigma}\right)^2} \end{cases} \quad (16)$$

$$(17)$$

with  $x_0 \in [0, L]$  the impact point on the beam and  $\sigma = 0.05L$ . This initial condition gives  $\phi_n = 0$ . The  $A_n$  parameter can be determined by :

$$A_n = \frac{1}{N_n \omega_n} \int_L \tilde{u}_n g \text{ with } N_n^2 = \int_L \tilde{u}_n^2 \quad (18)$$

Using Equations 15 and 18, we can generate a vibration pattern associated with an impact at the position  $x_0$  on the rod. We consider that the vibration  $v(x_0, t)$  which is perceived on the vertical axis by the user's hand can be approximated by (see Figure 1):

$$v(x_0, t) = u(x_h, t) \text{ with } x_h = 0.15L \quad (19)$$

The Figure 2 shows the contribution  $A_n(x_0)$  of each mode  $n$  for different impact position  $x_0$  along the rod.

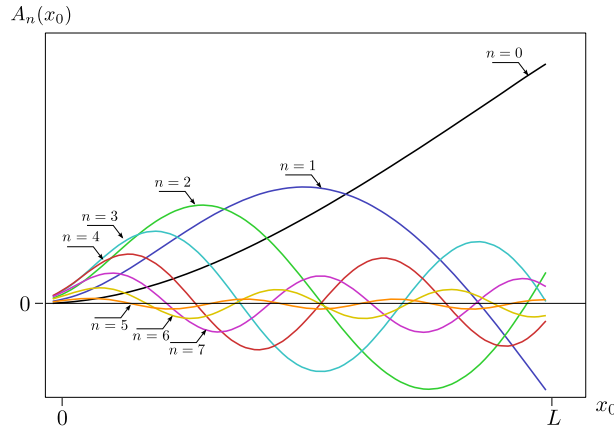


**Fig. 2.**  $A_n(x_0)$  for different impact positions  $x_0$

Even if the human hand is able to differentiate some complex vibrations, the signal generated by this model may be difficult to perceive or interpret. In the following section, we present some simplified patterns that can also be used to convey impact position information.

### 3.2 Simplified patterns

Using the Equations of the previous section on the Euler-Bernoulli beam, we can elaborate a simplified pattern that roughly reproduces the behavior of a real rod.

As we can see in Figure 2, the first mode amplitude is monotonically increasing. We can use a simplified model following this behavior :

$$v(x_0, t) = (ax_0 + b)e^{-\delta t} \sin(\omega t) \quad (20)$$

with  $a$ ,  $\omega$  and  $\delta$  chosen according to the simulated material [7].

We can also use the frequency to convey distance information. According to Equation 7, the frequency of each mode depends only on the length  $L$  of the rod :  $\omega \propto 1/L^2$ . Thus, we propose a simplified model which is inaccurate according to the real behavior but conveys distance information associated to the length of a rod:

$$v(x_0, t) = e^{-\delta t} \sin(cd^{(L-x_0)}t) \quad (21)$$

with  $c, d$  chosen to maximize the frequency perception on the desired interval of  $x_0$ .

It is also possible to combine these two models to convey the information of distance using the amplitude (Equation 20) and the frequency (Equation 21). This redundancy can be expected to improve the user's perception.

$$v(x_0, t) = (ax_0 + b)e^{-\delta t} \sin(cd^{(L-x_0)}t) \quad (22)$$

In the following section, we present a preliminary evaluation conducted to assess the user performance on each of these vibration patterns on a simple task.

## 4 Evaluation

### 4.1 Subjects

15 subjects (13 males, 2 females) aged between 23 and 57 (mean 29) years, one left-handed, participated in the experiment. All subjects were naive about the purpose of the experiment.

### 4.2 Experimental apparatus

A Virtuose6D device [5] was used to simulate the virtual horizontal rod held by the edge. The handle was constrained to a horizontal position and its movement constrained along the vertical axis. A virtual floor positioned at the base of the device was simulated using the standard haptic closed control loop. The control gains were set to have the most stiff and stable contact feedback as possible. The vibration was directly superimposed to the force feedback on the vertical axis (through the rotation of the handle around the fifth axis of the virtuose in order to avoid the bandwidth loss due to the mechanical system). The simulated rod

had no mass and no inertia. The vibration torque was triggered by the contact with the virtual floor and its amplitude was scaled according to the impact velocity. Six different vibration pattern models were tested. All the different models were scaled so that the maximum amplitude  $m = \max\{\|v(x_0, t)\|, x_0 \in [0, L], t \in \mathbb{R}^+\}$  of each model was the same. The maximum torque was set to 2 Nm. During the experiment, the subjects had to wear noise blocking headphones to eliminate any sound emitted by the haptic device.

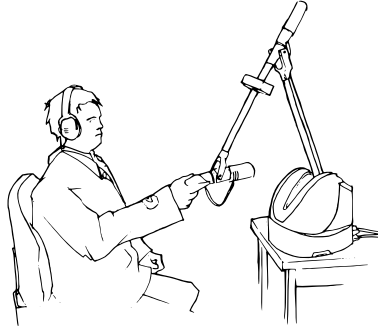


**Fig. 3.** Experimental apparatus

### 4.3 Vibration models

Six different vibration models were tested :

**EB1** (Euler-Bernoulli 1) A Euler-Bernoulli model with the first mode frequency of 70Hz and the second around 400Hz.

**EB2** (Euler-Bernoulli 2) A Euler-Bernoulli model with the first mode frequency of 25Hz and the second around 150Hz (a more massive beam).

**Am** (Varying Amplitude) The model described by Equation 20 with a constant vibration frequency of 70Hz and scaled amplitudes from 0.1 to 0.9.

**Fr** (Varying Frequency) The model described by Equation 21 with scaled frequencies from 270Hz to 100Hz and a constant amplitude of 0.5.

**AmFr** (Varying Amplitude and Frequency) The model described by Equation 22 using the same parameters as the two models *Am* and *Fr* : scaled amplitudes from 0.1 to 0.9 and scaled frequencies from 270Hz to 100Hz.

**AmCFr** (Conflicting variations of Amplitude and Frequency) In order to test which cue is dominant between amplitude and frequency we used a conflict situation. We combined *Am* with the inverted response of *Fr*  $x'_0 = L - x_0$  using  $v(x_0, t) = (ax_0 + b)e^{-\delta t} \sin(cd^{x_0}t)$ . The parameters are similar with the model *AmFr* with scaled amplitudes from 0.1 to 0.9 and *inverted* scaled frequencies from 100Hz to 270Hz.

### 4.4 Procedure

The subjects were told that they manipulated a horizontal rod held by one edge which was represented by the virtuose handle moving only on the vertical axis.

They were then required to hit the virtual floor only twice using their dominant hand and were told that each impact would occur at different locations of the rod. The subjects had then to choose with the buttons on the virtuouse handle which one of the two impacts was the farther one along the rod. The two impact locations were chosen among 4 predefined locations equally spread along the rod. All the 12 couples of locations were tested 8 times in a random order (see Figure 4).

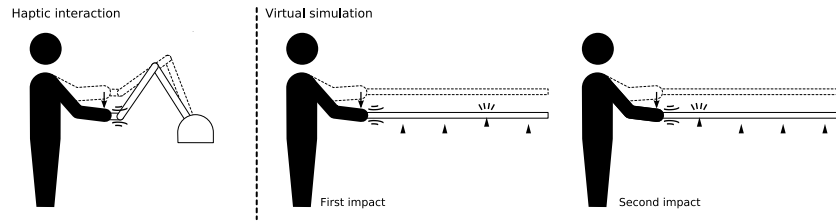


Fig. 4. Experimental procedure

All subjects tested the 96 couples of locations successively for each of the six vibration models in a balanced order to minimize any learning effect. At the end of the 576 trials, they were asked to rate the different vibration models from 1 to 7 according to the impact realism. They were also asked what strategy they used to choose the farther impact. At all time, the subjects were left naive about the different models they tested not to influence their judgment.

#### 4.5 Results

The proportion  $r$  of correct responses was evaluated for each participant for each model. A proportion  $r$  around 0.5 means that the subject was unable to associate the vibration pattern with an impact location. A proportion  $r$  over 0.75 indicates that the subject was able to make the correct association whereas a proportion  $r$  below 0.25 indicates that the subject was able to make an association but in the opposite way (*inverted* interpretation). To have an overall measure of the capacity of the subjects to associate the vibration in one way or another with a location, we use the value  $r' = |r - 0.5|$ . The results reported in Table 1 shows that the models  $Am$  (varying amplitude with constant frequency) and  $Fr$  (varying frequency with constant amplitude) are achieving the highest performance among subjects. The one-way repeated measures ANOVA (Huynh and Feldt adjusted) among subjects was found significant ( $F(5) = 3.47, p < 0.007$ ). The non-parametric Friedman ANOVA was also found significant ( $\chi^2 = 22.1, \text{dof} = 5, p < 0.0005$ ). The paired  $t$ -test on  $r$  was found significant ( $p < 0.05$ ) between the models  $Am$  - ( $EB1, EB2, AmCFr$ ) and  $Fr$  - ( $EB1, EB2$ ).

The percentage of inverted interpretations (*inversion ratio*) is reported in Table 1. This ratio was evaluated by considering the number of subjects making the association between vibration and location in the right way and the number



of subjects making the association in the opposite way. The model *EB1* (Euler-Bernoulli model) is the less often inverted model among the subjects, followed by *Fr*. Correlation tests showed that models *Fr* and *AmCFr* were strongly correlated ( $r(15) = -0.70, p < 0.004$ ).

The results of the subjective rating of impact realism are also reported in Table 1. The model *EB2* (Euler-Bernoulli model of a massive beam) was preferred in terms of impact realism. The one-way repeated measures ANOVA among subjects was found significant ( $F(5) = 4.62, p < 0.0014$ ). The non-parametric Friedman ANOVA was also found significant ( $\chi^2 = 14.3, \text{dof} = 5, p < 0.014$ ). The paired *t*-test on ratings was found significant ( $p < 0.05$ ) between the models *Am* - (*EB1, EB2, Fr, AmFr*) and *EB2* - (*Fr, AmCFr*).

Model		EB1	EB2	Am	Fr	AmFr	AmCFr
$r'$	<i>m</i>	0.25	0.22	0.34	0.32	0.28	0.27
	$\sigma$	0.13	0.13	0.1	0.14	0.13	0.12
Realism ratings	<i>m</i>	4.83	5.58	3.25	4.67	5	4.5
	$\sigma$	1.03	1.08	1.86	1.23	1.48	1.45
Inversion ratio	%	25	50	54	31	39	65

**Table 1.** Mean and standard deviation of  $r' = |r - 0.5|$  (representing the overall performance) and of the subjective rating of realism for the six vibration models. The last line represents the percentage of inverted interpretations (*inversion* ratio) for each model.

## 5 Discussion

Our results show that with all the vibration models tested, the subjects were able to associate an impact location with a vibration pattern. The most simplified vibration models (*Am* and *Fr*) seem to be interpreted more easily than the more complex ones (*EB1* and *EB2*). The correlation between models *AmCFr* and *Fr* suggests that the subjects relied mainly on the frequency cue when there is a conflict situation.

The number of subjects that interpreted the vibration model in the opposite way was the lowest for models *EB1* and *Fr*. This result suggests that the perception of the impact location using frequencies may be more consistent among the subjects (less prone to be inverted). The model *Fr* is physically inaccurate for a constant length rod and rather describes the behavior of rods of different lengths. This behavior may be more easily depicted by the subjects than the original task. The main difference between the models *EB1* and *EB2* is the dispersion of vibrational modes. The first two modes of the *EB1* model may be perceived more easily than those of the *EB2* model which are mixed with higher order modes in the tactile perception bandwidth. The perception of these first two modes may allow the subject to give a more consistent interpretation of the impact location. Further work is however required to test these two hypotheses.

Taken together, our results suggest that the model  $Fr$  (frequency changes) may be a good compromise between realism and performance.

In this preliminary evaluation, the hand impedance and the resulting output bandwidth of the haptic device was not evaluated. Further work is required to measure and investigate the effects of these parameters.

## 6 Conclusion and future work

We presented in this paper different vibration pattern models to convey the impact position information: a realistic model based on a numerical simulation of a beam and simplified models based on exponentially decaying sinusoids. A preliminary evaluation has been conducted on six different vibration models. Taken together, the results showed that the user is able to associate vibration information with impact position using these models. Further work will first consist in deeper analysis of the data and investigations of the different interpretations of each vibration model and the user's strategies adopted. Afterwards, we would also like to investigate the role of the hand impedance and the effects of the haptic output bandwidth to elaborate more effective vibration pattern models.

## References

1. S. J. Bensmaïa and M. Hollins. Complex tactile waveform discrimination. *The Journal of the Acoustical Society of America*, 108(3):1236–1245, 2000.
2. S. J. Bolanowsky Jr, G. A. Gescheider, R. T. Verrillo, and C. M. Checkosky. Four channels mediate the mechanical aspects of touch. *The Journal of the Acoustical Society of America*, 84(5):1680–1694, 1988.
3. T.-C. Chan. The situational effects on haptic perception of rod length. *Perception & Psychophysics*, 58(7):1110–1123, 1996.
4. J. T. Dennerlein, P. A. Millman, and R. D. Howe. Vibrotactile feedback for industrial telemanipulators. In *Proceedings of the ASME Dynamic Control Division*, pages 189–195, 1997.
5. Haption. Haption Virtuose 6D35-45 technical specifications. <http://www.haption.com>, 2003.
6. K. J. Kuchenbecker, J. Fiene, and G. Niemeyer. Improving contact realism through event-based haptic feedback. *IEEE Transactions on Visualization and Computer Graphics*, 12(2):219–230, 2006.
7. A. M. Okamura, J. T. Dennerlein, and R. D. Howe. Vibration feedback models for virtual environments. In *Proceedings of IEEE International Conference on Robotics and Automation*, volume 1, pages 674–679, 1998.
8. A. M. Okamura, M. W. Hage, J. T. Dennerlein, and M. R. Cutkosky. Reality-based models for vibration feedback in virtual environments. *IEEE ASME Transactions on Mechatronics*, 6(2):245–252, 2001.
9. P. Wellman and R. D. Howe. Towards realistic vibrotactile display in virtual environments. In *Proceeding of the ASME Dynamics Systems and Control Division*, volume 57, 1995.
10. H.-Y. Yao and V. Hayward. An experiment on length perception with a virtual rolling stone. In *Proceedings of Eurohaptics*, pages 325–330, 2006.